Probing near Dirac point electron-phonon interaction in graphene

Jingzhi Shang,[1,*] Suxia Yan,[2] Chunxiao Cong,[1] Howe-Siang Tan,[1,2] Ting Yu,[1,3,4] and Gagik G. Gurzadyan[1]

[1]*Division of Physics and Applied Physics, School of Physical and Mathematical Sciences, Nanyang Technological University, Singapore 637371, Singapore*
[2]*Division of Chemistry and Biological Chemistry, School of Physical and Mathematical Sciences, Nanyang Technological University, Singapore 637371, Singapore*
[3]*Department of Physics, Faculty of Science, National University of Singapore, Singapore 117542, Singapore*
[4]*Graphene Research Centre, National University of Singapore, 2 Science Drive 3, Singapore 117542, Singapore*
**s090029@e.ntu.edu.sg*

Abstract: Carrier dynamics in graphene films on CaF_2 have been measured in the mid infrared region by femtosecond pump-probe spectroscopy. The relaxation kinetics shows two decay times. The fast time component is ~0.2 ps, which is attributed to the mixture of initial few ultrafast intraband and interband decay channels. The slow component is ~1.5 ps, which is primarily assigned to optical phonon-acoustic phonon scattering. The contribution of fast component exhibits an increase trend in the probe photon frequencies from 2600 to 3100 cm^{-1}. At the probe frequency of 2700 cm^{-1}, the accelerated carrier relaxation was detected, which resulted from the interband triple-resonance electron-phonon scattering in graphene. At the probe frequency of 3175 cm^{-1}, a clear instant negative differential transmission signal was observed, which is due to stimulated two-phonon emission involved with G phonons in graphene. This result indicates that graphene can be used as a source of coherent ultrashort sound-wave emission.

OCIS codes: (320.7130) Ultrafast processes in condensed matter, including semiconductors; (320.7110) Ultrafast nonlinear optics; (160.4236) Nanomaterials.

References and links

1. A. K. Geim, "Graphene: status and prospects," Science **324**(5934), 1530–1534 (2009).
2. K. S. Novoselov, "Nobel lecture: graphene: materials in the flatland," Rev. Mod. Phys. **83**(3), 837–849 (2011).
3. A. H. Castro Neto, N. M. R. Peres, K. S. Novoselov, and A. K. Geim, "The electronic properties of graphene," Rev. Mod. Phys. **81**(1), 109–162 (2009).
4. S. Das Sarma, S. Adam, E. H. Hwang, and E. Rossi, "Electronic transport in two-dimensional graphene," Rev. Mod. Phys. **83**(2), 407–470 (2011).
5. E. H. Hwang, B. Y.-K. Hu, and S. Das Sarma, "Inelastic carrier lifetime in graphene," Phys. Rev. B **76**(11), 115434 (2007).
6. C.-H. Park, F. Giustino, M. L. Cohen, and S. G. Louie, "Velocity renormalization and carrier lifetime in graphene from the electron-phonon interaction," Phys. Rev. Lett. **99**(8), 086804 (2007).
7. J. González and E. Perfetto, "Unconventional quasiparticle lifetime in graphene," Phys. Rev. Lett. **101**(17), 176802 (2008).
8. R. Kim, V. Perebeinos, and P. Avouris, "Relaxation of optically excited carriers in graphene," Phys. Rev. B **84**(7), 075449 (2011).
9. J. Shang, Z. Luo, C. Cong, J. Lin, T. Yu, and G. G. Gurzadyan, "Femtosecond UV-pump/visible-probe measurements of carrier dynamics in stacked graphene films," Appl. Phys. Lett. **97**(16), 163103 (2010).
10. J. Shang, T. Yu, and G. G. Gurzadyan, "Femtosecond energy relaxation in suspended graphene: phonon-assisted spreading of quasiparticle distribution," Appl. Phys. B **107**(1), 131–136 (2012).
11. Q. Bao, H. Zhang, Z. Ni, Y. Wang, L. Polavarapu, Z. Shen, Q.-H. Xu, D. Tang, and K. P. Loh, "Monolayer graphene as a saturable absorber in a mode-locked laser," Nano Res. **4**(3), 297–307 (2011).
12. F. Carbone, G. Aubock, A. Cannizzo, F. Van Mourik, R. R. Nair, A. K. Geim, K. S. Novoselov, and M. Chergui, "Femtosecond carrier dynamics in bulk graphite and graphene paper," Chem. Phys. Lett. **504**(1-3), 37–40 (2011).
13. J. Shang, T. Yu, J. Lin, and G. G. Gurzadyan, "Ultrafast electron-optical phonon scattering and quasiparticle lifetime in CVD-grown graphene," ACS Nano **5**(4), 3278–3283 (2011).

#176199 - $15.00 USD Received 13 Sep 2012; revised 18 Oct 2012; accepted 21 Oct 2012; published 5 Nov 2012

14. M. Breusing, S. Kuehn, T. Winzer, E. Malic, F. Milde, N. Severin, J. P. Rabe, C. Ropers, A. Knorr, and T. Elsaesser, "Ultrafast nonequilibrium carrier dynamics in a single graphene layer," Phys. Rev. B **83**(15), 153410 (2011).
15. J. M. Dawlaty, S. Shivaraman, M. Chandrashekhar, F. Rana, and M. G. Spencer, "Measurement of ultrafast carrier dynamics in epitaxial graphene," Appl. Phys. Lett. **92**(4), 042116 (2008).
16. L. Huang, G. V. Hartland, L.-Q. Chu, R. M. Luxmi, R. M. Feenstra, C. Lian, K. Tahy, and H. Xing, "Ultrafast transient absorption microscopy studies of carrier dynamics in epitaxial graphene," Nano Lett. **10**(4), 1308–1313 (2010).
17. H. Wang, J. H. Strait, P. A. George, S. Shivaraman, V. B. Shields, M. Chandrashekhar, J. Hwang, F. Rana, M. G. Spencer, C. S. Ruiz-Vargas, and J. Park, "Ultrafast relaxation dynamics of hot optical phonons in graphene," Appl. Phys. Lett. **96**(8), 081917 (2010).
18. B. Gao, G. Hartland, T. Fang, M. Kelly, D. Jena, H. G. Xing, and L. Huang, "Studies of intrinsic hot phonon dynamics in suspended graphene by transient absorption microscopy," Nano Lett. **11**(8), 3184–3189 (2011).
19. P. J. Hale, S. M. Hornett, J. Moger, D. W. Horsell, and E. Hendry, "Hot phonon decay in supported and suspended exfoliated graphene," Phys. Rev. B **83**(12), 121404 (2011).
20. P. A. Obraztsov, M. G. Rybin, A. V. Tyurnina, S. V. Garnov, E. D. Obraztsova, A. N. Obraztsov, and Y. P. Svirko, "Broadband light-induced absorbance change in multilayer graphene," Nano Lett. **11**(4), 1540–1545 (2011).
21. D. Sun, Z.-K. Wu, C. Divin, X. Li, C. Berger, W. A. de Heer, P. N. First, and T. B. Norris, "Ultrafast relaxation of excited Dirac fermions in epitaxial graphene using optical differential transmission spectroscopy," Phys. Rev. Lett. **101**(15), 157402 (2008).
22. K.-J. Yee, J.-H. Kim, M. H. Jung, B. H. Hong, and K.-J. Kong, "Ultrafast modulation of optical transitions in monolayer and multilayer graphene," Carbon **49**(14), 4781–4785 (2011).
23. D. Sun, C. Divin, C. Berger, W. A. de Heer, P. N. First, and T. B. Norris, "Hot carrier cooling by acoustic phonons in epitaxial graphene by ultrafast pump-probe spectroscopy," Phys. Status Solidi C **8**(4), 1194–1197 (2011).
24. T. Limmer, A. J. Houtepen, A. Niggebaum, R. Tautz, and E. Da Como, "Influence of carrier density on the electronic cooling channels of bilayer graphene," Appl. Phys. Lett. **99**(10), 103104 (2011).
25. S. Winnerl, M. Orlita, P. Plochocka, P. Kossacki, M. Potemski, T. Winzer, E. Malic, A. Knorr, M. Sprinkle, C. Berger, W. A. de Heer, H. Schneider, and M. Helm, "Carrier relaxation in epitaxial graphene photoexcited near the Dirac point," Phys. Rev. Lett. **107**(23), 237401 (2011).
26. P. A. George, J. Strait, J. Dawlaty, S. Shivaraman, M. Chandrashekhar, F. Rana, and M. G. Spencer, "Ultrafast optical-pump terahertz-probe spectroscopy of the carrier relaxation and recombination dynamics in epitaxial graphene," Nano Lett. **8**(12), 4248–4251 (2008).
27. H. Choi, F. Borondics, D. A. Siegel, S. Y. Zhou, M. C. Martin, A. Lanzara, and R. A. Kaindl, "Broadband electromagnetic response and ultrafast dynamics of few-layer epitaxial graphene," Appl. Phys. Lett. **94**(17), 172102 (2009).
28. J. H. Strait, H. Wang, S. Shivaraman, V. Shields, M. Spencer, and F. Rana, "Very slow cooling dynamics of photoexcited carriers in graphene observed by optical-pump terahertz-probe spectroscopy," Nano Lett. **11**(11), 4902–4906 (2011).
29. A. Bostwick, T. Ohta, T. Seyller, K. Horn, and E. Rotenberg, "Quasiparticle dynamics in graphene," Nat. Phys. **3**(1), 36–40 (2007).
30. S. Y. Zhou, G.-H. Gweon, A. V. Fedorov, P. N. First, W. A. de Heer, D.-H. Lee, F. Guinea, A. H. Castro Neto, and A. Lanzara, "Substrate-induced bandgap opening in epitaxial graphene," Nat. Mater. **6**(10), 770–775 (2007).
31. Y. Liu, L. Zhang, M. K. Brinkley, G. Bian, T. Miller, and T.-C. Chiang, "Phonon-induced gaps in graphene and graphite observed by angle-resolved photoemission," Phys. Rev. Lett. **105**(13), 136804 (2010).
32. D. A. Siegel, C.-H. Park, C. Hwang, J. Deslippe, A. V. Fedorov, S. G. Louie, and A. Lanzara, "Many-body interactions in quasi-freestanding graphene," Proc. Natl. Acad. Sci. U.S.A. **108**(28), 11365–11369 (2011).
33. R. R. Nair, P. Blake, A. N. Grigorenko, K. S. Novoselov, T. J. Booth, T. Stauber, N. M. R. Peres, and A. K. Geim, "Fine structure constant defines visual transparency of graphene," Science **320**(5881), 1308 (2008).
34. L. M. Malard, M. A. Pimenta, G. Dresselhaus, and M. S. Dresselhaus, "Raman spectroscopy in graphene," Phys. Rep. **473**(5-6), 51–87 (2009).
35. R. Saito, M. Hofmann, G. Dresselhaus, A. Jorio, and M. S. Dresselhaus, "Raman spectroscopy of graphene and carbon nanotubes," Adv. Phys. **60**(3), 413–550 (2011).
36. A. Gupta, G. Chen, P. Joshi, S. Tadigadapa, and P. C. Eklund, "Raman scattering from high-frequency phonons in supported n-graphene layer films," Nano Lett. **6**(12), 2667–2673 (2006).
37. Z. Ni, Y. Wang, T. Yu, and Z. Shen, "Raman spectroscopy and imaging of graphene," Nano Res. **1**(4), 273–291 (2008).
38. F. Rana, "Electron-hole generation and recombination rates for coulomb scattering in graphene," Phys. Rev. B **76**(15), 155431 (2007).
39. F. Rana, P. A. George, J. H. Strait, J. Dawlaty, S. Shivaraman, M. Chandrashekhar, and M. Spencer, "Carrier recombination and generation rates for intravalley and intervalley phonon scattering in graphene," Phys. Rev. B **79**(11), 115447 (2009).
40. K. M. Borysenko, J. T. Mullen, E. A. Barry, S. Paul, Y. G. Semenov, J. M. Zavada, M. B. Nardelli, and K. W. Kim, "First-principles analysis of electron-phonon interactions in graphene," Phys. Rev. B **81**(12), 121412 (2010).
41. T. Winzer, A. Knorr, and E. Malic, "Carrier multiplication in graphene," Nano Lett. **10**(12), 4839–4843 (2010).

#176199 - $15.00 USD Received 13 Sep 2012; revised 18 Oct 2012; accepted 21 Oct 2012; published 5 Nov 2012

42. F. Rana, J. H. Strait, H. Wang, and C. Manolatou, "Ultrafast carrier recombination and generation rates for plasmon emission and absorption in graphene," Phys. Rev. B **84**(4), 045437 (2011).
43. E. Malic, T. Winzer, E. Bobkin, and A. Knorr, "Microscopic theory of absorption and ultrafast many-particle kinetics in graphene," Phys. Rev. B **84**(20), 205406 (2011).
44. A. L. Walter, A. Bostwick, K.-J. Jeon, F. Speck, M. Ostler, T. Seyller, L. Moreschini, Y. J. Chang, M. Polini, R. Asgari, A. H. MacDonald, K. Horn, and E. Rotenberg, "Effective screening and the plasmaron bands in graphene," Phys. Rev. B **84**(8), 085410 (2011).
45. K. Kang, D. Abdula, D. G. Cahill, and M. Shim, "Lifetimes of optical phonons in graphene and graphite by time-resolved incoherent anti-Stokes Raman scattering," Phys. Rev. B **81**(16), 165405 (2010).
46. W.-K. Tse and S. Das Sarma, "Energy relaxation of hot Dirac fermions in graphene," Phys. Rev. B **79**(23), 235406 (2009).
47. Z. Luo, T. Yu, J. Shang, Y. Wang, S. Lim, L. Liu, G. G. Gurzadyan, Z. Shen, and J. Lin, "Large-scale synthesis of bi-Layer graphene in strongly coupled stacking order," Adv. Funct. Mater. **21**(5), 911–917 (2011).
48. C. Thomsen and S. Reich, "Double resonant raman scattering in graphite," Phys. Rev. Lett. **85**(24), 5214–5217 (2000).
49. I. Kupčic, "Triple-resonant two-phonon Raman scattering in graphene," J. Raman Spectrosc. **43**(1), 1–5 (2012).
50. J. Kürti, V. Zolyomi, A. Gruneis, and H. Kuzmany, "Double resonant Raman phenomena enhanced by Van Hove singularities in single-wall carbon nanotubes," Phys. Rev. B **65**(16), 165433 (2002).
51. S. Wu, L. Jing, Q. Li, Q. W. Shi, J. Chen, H. Su, X. Wang, and J. Yang, "Average density of states in disordered graphene systems," Phys. Rev. B **77**(19), 195411 (2008).
52. K. S. Novoselov, A. K. Geim, S. V. Morozov, D. Jiang, M. I. Katsnelson, I. V. Grigorieva, S. V. Dubonos, and A. A. Firsov, "Two-dimensional gas of massless Dirac fermions in graphene," Nature **438**(7065), 197–200 (2005).
53. J. Martin, N. Akerman, G. Ulbricht, T. Lohmann, J. H. Smet, K. von Klitzing, and A. Yacoby, "Observation of electron–hole puddles in graphene using a scanning single-electron transistor," Nat. Phys. **4**(2), 144–148 (2008).
54. Y. Zhang, V. W. Brar, C. Girit, A. Zettl, and M. F. Crommie, "Origin of spatial charge inhomogeneity in graphene," Nat. Phys. **5**(10), 722–726 (2009).
55. K. Ziegler, B. Dóra, and P. Thalmeier, "Density of states in disordered graphene," Phys. Rev. B **79**(23), 235431 (2009).
56. R. Xiao, F. Tasnadi, K. Koepernik, J. W. F. Venderbos, M. Richter, and M. Taut, "Density functional investigation of rhombohedral stacks of graphene: topological surface states, nonlinear dielectric response, and bulk limit," Phys. Rev. B **84**(16), 165404 (2011).
57. B. A. Ruzicka, S. Wang, J. Liu, K.-P. Loh, J. Z. Wu, and H. Zhao, "Spatially resolved pump-probe study of single-layer graphene produced by chemical vapor deposition," Opt. Mater. Express **2**(6), 708–716 (2012).
58. W. E. Bron and W. Grill, "Stimulated phonon emission," Phys. Rev. Lett. **40**(22), 1459–1463 (1978).
59. P. Hu, "Stimulated emission of 29-cm^{-1} phonons in ruby," Phys. Rev. Lett. **44**(6), 417–420 (1980).
60. L. G. Tilstra, A. F. M. Arts, and H. W. de Wijn, "Coherence of phonon avalanches in ruby," Phys. Rev. B **68**(14), 144302 (2003).
61. L. G. Tilstra, A. F. M. Arts, and H. W. de Wijn, "Optically excited ruby as a saser: experiment and theory," Phys. Rev. B **76**(2), 024302 (2007).
62. K. Vahala, M. Herrmann, S. Knünz, V. Batteiger, G. Saathoff, T. W. Hänsch, and T. Udem, "A phonon laser," Nat. Phys. **5**(9), 682–686 (2009).
63. P. M. Walker, A. J. Kent, M. Henini, B. A. Glavin, V. A. Kochelap, and T. L. Linnik, "Terahertz acoustic oscillations by stimulated phonon emission in an optically pumped superlattice," Phys. Rev. B **79**(24), 245313 (2009).
64. R. P. Beardsley, A. V. Akimov, M. Henini, and A. J. Kent, "Coherent terahertz sound amplification and spectral line narrowing in a stark ladder superlattice," Phys. Rev. Lett. **104**(8), 085501 (2010).
65. I. S. Grudinin, H. Lee, O. Painter, and K. J. Vahala, "Phonon laser action in a tunable two-level system," Phys. Rev. Lett. **104**(8), 083901 (2010).
66. T. Winzer, E. Malic, and A. Knorr, "Microscopic mechanism for transient population inversion and optical gain in graphene," arXiv:1209.4833v1 (Sep 21, 2012), http://arxiv.org/abs/1209.4833.
67. T. Li, L. Luo, M. Hupalo, J. Zhang, M. C. Tringides, J. Schmalian, and J. Wang, "Femtosecond population inversion and stimulated emission of dense Dirac fermions in graphene," Phys. Rev. Lett. **108**(16), 167401 (2012).
68. S. Yan, M. T. Seidel, Z. Zhang, W. K. Leong, and H.-S. Tan, "Ultrafast vibrational relaxation dynamics of carbonyl stretching modes in $Os_3(CO)_{12}$," J. Chem. Phys. **135**(2), 024501 (2011).
69. S. Ullrich, T. Schultz, M. Z. Zgierski, and A. Stolow, "Electronic relaxation dynamics in DNA and RNA bases studied by time-resolved photoelectron spectroscopy," Phys. Chem. Chem. Phys. **6**(10), 2796–2801 (2004).

1. Introduction

Graphene, two-dimensional carbon, has aroused great attention from both scientific and industrial communities. Their unique properties [1,2] and promising applications [2] strongly rely on the electronic structure with a linear dispersion around Dirac point [3]. In particular, investigation of carrier dynamics in graphene is very important for testing the concepts of fundamental physics and understanding electron-electron (e-e) and electron-phonon (e-p)

#176199 - $15.00 USD Received 13 Sep 2012; revised 18 Oct 2012; accepted 21 Oct 2012; published 5 Nov 2012

scattering processes in two-dimensional materials. Nowadays, graphene-based electronic devices have shown many promising applications, however, origins of some electron transport behaviors in these devices are still controversial [2,4]. To clarify these electron properties, it is necessary to understand the carrier scattering processes in the low-energy regions near Dirac point. Theoretically, the energy dependences of carrier dynamics have been predicted by considering various possible relaxation channels [5–8]. On the other hand, ultrafast laser [9–28] and angle-resolved photoemission spectroscopic studies [29–32] on graphene films have experimentally provided a great deal of information of carrier dynamics. Especially, ultrafast pump-probe technique has been extensively used to study carrier dynamics, i.e. the real-time quasiparticle relaxation, by adjusting the time delay between pump and probe pulses. Previously, most ultrafast pump-probe studies on carrier dynamics in graphene films have been reported in the visible [9–14], near infrared (NIR: 0.75-3 μm) [11–25], mid IR (MIR: 3-50 μm) [24,25], and far IR (FIR: 50-1000 μm) [25–28] probe regions. Only few studies [24,25] on the carrier dynamics of graphene films have been done in the MIR region.

In this work, femtosecond pump/probe measurements of graphene films have been performed in the MIR probe region from 3.15 to 5.0 μm (probe photon frequencies: 2000-3175 cm^{-1}). The carrier relaxation exhibits biexponential decay. One is the superposition of several ultrafast decay channels. The other is mainly caused by optical phonon-acoustic phonon (op-ap) scattering. The frequency-dependent carrier relaxation was examined. For the first time, anomalous carrier decay processes were observed at the probe frequencies of 2700 cm^{-1} and 3175 cm^{-1}. Their possible origins are discussed by analyzing the related optical phonons.

2. Results and discussion

Figure 1 shows typical transmission and Raman spectra of graphene films on CaF_2 wafer. Previous studies [33] indicate that the opacity of graphene films is quantized and the value is 2.3% for monolayer graphene. In our case, the transmittance of the graphene films at 600 nm is about 70% as shown in Fig. 1(a); the estimated number of graphene layers is ~15. Furthermore, the transmission spectrum was also measured in the range from NIR to MIR (Fig. 1(b)). All over the range between 1200 and 7500 cm^{-1}, transmission is about 70-75%. Weak IR absorption bands are assigned to -C = C- (~1540 and ~1640 cm^{-1}), CH_2 (~2861 and ~2925 cm^{-1}) and C-H (~3298 cm^{-1}) vibrations. These vibrational modes are probably from the defect and/or edge sites in stacked graphene films. In the following transient pump-probe measurements, probe frequencies were selected (as denoted by the black arrows) in order not to match above vibrational modes. For Raman measurements, sixty Raman spectra were collected from the different regions of graphene films on CaF_2 substrate (Figs. 1(c) and 1(d)): peak positions of G and G′ bands are located at 1584 ± 1 and 2690 ± 2 cm^{-1}, respectively. The corresponding FWHMs of G and G′ bands are 20 ± 2 and 41 ± 3 cm^{-1}, respectively. It is well known that Raman spectra are sensitive to the electronic structure [34,35]. The Raman features of this sample are close to that of monolayer graphene rather than those from Bernal stacked graphene multilayers [36,37]. Therefore, most intrinsic properties of monolayer graphene were expected to be preserved in the used graphene films.

#176199 - $15.00 USD Received 13 Sep 2012; revised 18 Oct 2012; accepted 21 Oct 2012; published 5 Nov 2012

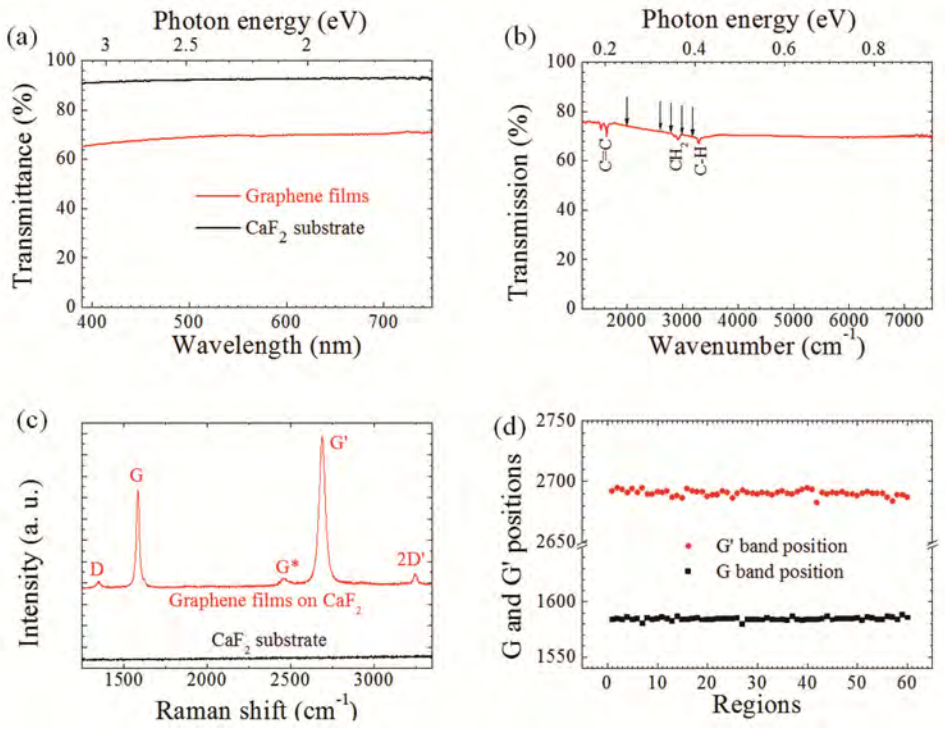

Fig. 1. (a, b) Transmission and (c, d) Raman data of graphene films on CaF_2 substrate.

Figure 2 presents the differential transmission (ΔT/T) kinetics as a function of delay time by using the degenerate MIR pump-probe at ν = 2000 cm^{-1}:$\Delta T = T_{with\ pump}-T_{without\ pump}$. The positive decay curve was well fitted by two exponential functions convoluted with the instrument response function. The fast and slow components are ~0.2 and ~1.0 ps with the fractional amplitudes of 64% and 36%, respectively. Due to the symmetric linear energy dispersion, the probed electron energy level at 0.124 eV above Dirac energy is half of the probe phonon energy [3,4], which is less than the energy of either zone-boundary/edge optical phonon (~0.167 eV) around K (K′) point or zone-center optical phonon (~0.196 eV) around Γ point [34–36]. Thus, the intraband optical phonon emission, the dominant energy relaxation process for the visible photon probe regions [9–13], can be excluded for the observed decay. Here, the fast decay is assigned to the mixture of initial few ultrafast intraband and interband scattering mechanisms [8,29,38–44], which include the intraband e-e scattering and interband electron-optical phonon (e-op) scattering and may involve electron-plasmon scattering [8,29,42–44], interband Auger recombination and impact ionization [38,39,41,43].

The slow component of 1 ps was attributed to op-ap scattering and this time scale agrees well with optical phonon lifetimes in previous reports [13,15,16,18–20,45]. The very slow electron-acoustic phonon scattering (e-ac) was not observed in our room temperature measurements. The result is consistent with the recent studies [25,28], where the long decay times of tens to hundreds of ps were substrate temperature dependent and only observed in the low temperature pump-probe measurements. Moreover, the theoretical calculations [46] of temperature dependent carrier relaxation support current observation, where the e-op (or e-ac) scattering becomes dominant when the electron temperature is more (or less) than 200-300 K. In addition, this measurement indicates that the Fermi level of the sample is within ± 0.124 eV referring to the Dirac energy. If the sample is strongly electron/hole doped and the Fermi level is higher (lower) than + 0.124 eV (–0.124 eV), the induced transmission (ΔT/T) is expected to be 0 as the photon absorption is suppressed due to the Pauli blocking in the conduction band (CB)/the poor electron concentration in the valance band (VB).

#176199 - $15.00 USD Received 13 Sep 2012; revised 18 Oct 2012; accepted 21 Oct 2012; published 5 Nov 2012

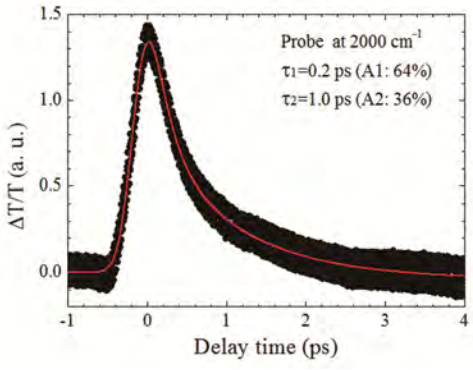

Fig. 2. Carrier dynamics of graphene films on CaF_2 by the degenerate MIR pump and probe configuration at 2000 cm^{-1}.

Figure 3(a) shows the ΔT/T spectra at four MIR probe frequencies obtained by the non-degenerate 800 nm pump/MIR probe configuration. It is clear that the carrier relaxation becomes slower at low probe frequencies in the range between 2600 and 3100 cm^{-1}. Performing biexponential fit of the decay curves, the lifetimes and fractional amplitudes versus the electron energy and/or the probe phonon frequency were obtained (Fig. 3(b)). Two time scales were extracted as above: ultrafast processes are 0.2 ± 0.1 ps and the slower ones of 1.5 ± 0.2 ps. The fractional amplitude of the fast/slow component increases/decreases versus the electron energy (half of the probe photon energy). Besides, for the probe photon frequency at 2600 cm^{-1}, the origin of the fast decay is similar to that in Fig. 2. For the other three frequencies, intraband zone-boundary optical phonon emission is allowed, which partially contributes to the ultrafast decay, in contrast to ν = 2000 cm^{-1}, where interband zone-boundary optical phonon emission takes place. Previously, decay of 4 ps for exfoliated *bilayer* graphene was reported at the probe energy of 0.3 eV [24], which is slightly larger than our results on *stacked* graphene layers. The difference is attributed to the energy band splitting in bilayer graphene, which slows down the carrier relaxation [47].

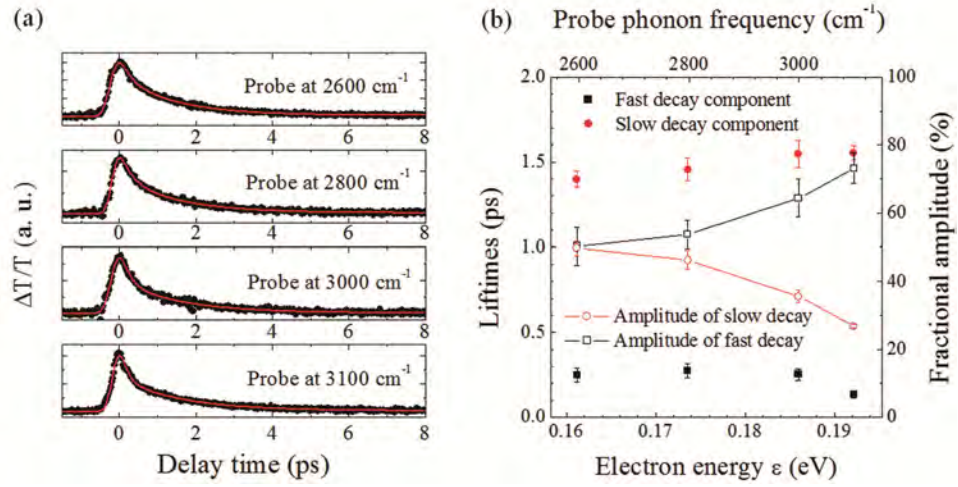

Fig. 3. (a) Frequency-dependent carrier dynamics of graphene films on CaF_2, λ_{exc} = 800 nm; (b) the energy dependence of fitting parameters of carrier lifetimes.

Figure 4(a) presents the carrier dynamics measured at λ_{exc} = 800 nm and probed at λ_{pr} = 3.7 μm (ν = 2700 cm^{-1}). This probe frequency corresponds to the G′ band as shown in Fig. 4(b). Figure 4(c) shows the typical double resonance Raman scattering of G′. The fast decay

#176199 - $15.00 USD Received 13 Sep 2012; revised 18 Oct 2012; accepted 21 Oct 2012; published 5 Nov 2012

τ_1 is shorter than those probed at both sides (2600 and 2800 cm^{-1}) (Fig. 3(a)), and its contribution to $\Delta T/T$ is also larger. In other words, the carrier relaxation at this frequency is faster than those at neighboring frequencies. Different from the conventional intervalley e-op scattering [35,39,43] (Fig. 4(d)), the accelerated decay was attributed to the enhanced zone-boundary optical phonon emission (G′ band) due to intervalley triply *resonant* e-op scattering (Fig. 4(e)).

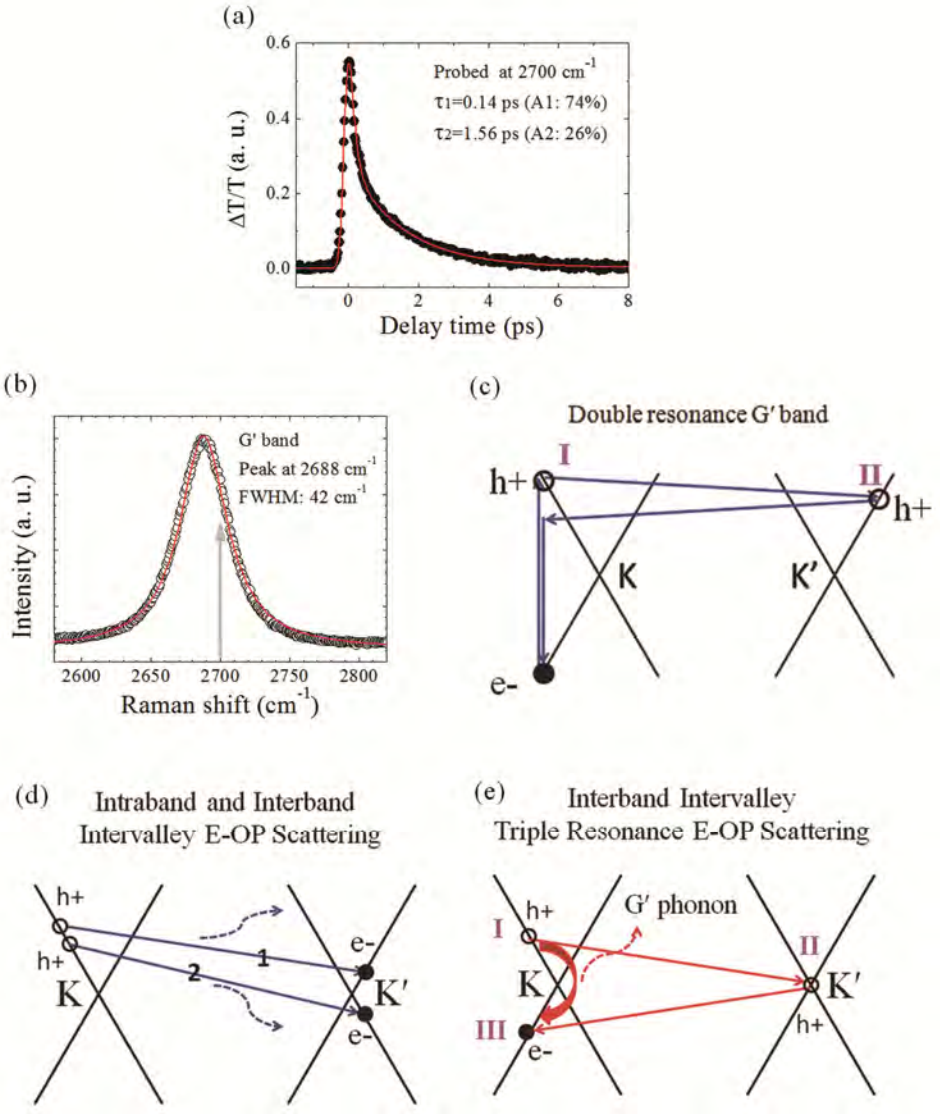

Fig. 4. (a) Carrier dynamics of graphene films at the probe frequency of 2700 cm^{-1} measured by the 800 nm pump/MIR probe setup; (b) Raman spectrum of G′ band of graphene films on CaF_2; (c) Schematic of double resonance scattering of G′ band; (d) Electron relaxation by intraband (1) and interband (2) intervalley e-op scattering processes; (e) Electron relaxation by triple resonance e-op scattering process in graphene films on CaF_2.

Note that the G′ band extensively investigated in previous studies [34,35,48] is normally caused by doubly resonant (DR) Raman scattering related to two real electronic states, I and II, as shown in Fig. 4(c). In our case, the formation of the triply resonant (TR) scattering is due to a new electronic state (III) involved at this specified probe frequency, where the second

#176199 - $15.00 USD Received 13 Sep 2012; revised 18 Oct 2012; accepted 21 Oct 2012; published 5 Nov 2012

phonon emission process is additionally resonant with this state III. Some studies show that the possible triply resonant processes of G′ band in graphene [49] and of D band in single-wall carbon nanotubes [50] are much intense than conventional doubly resonant scattering. The energy dissipation of excited electrons in graphene is mainly due to e-op scattering as discussed above. Therefore, it is expected that the stronger triply resonant e-op scattering will accelerate the relaxation of excited electrons at 2700 cm^{-1}. Indeed, the faster carrier relaxation (τ = 0.14 ps; A = 74%) by e-op scattering was observed in Fig. 4(a) than those (τ = 0.2-0.3 ps; A ≈50%) at nearby probe frequencies (at 2600 and 2800 cm^{-1} in Fig. 3).

Furthermore, it should be mentioned that the triply resonant scattering requires existence of some electronic states around Dirac point. In other words, the density of states around Dirac point should not be zero, as predicted for the ideal graphene [3,51]. Indeed, previous electronic transport studies [52–54] have clearly demonstrated that the carrier densities for graphene are not zero due to various reasons, such as disorders, charge impurity doping, inhomogeneous carrier distribution, etc. Meanwhile, by considering the inevitable disorder in graphene and stacked graphene films, the theoretical calculations also show that there is density of states around Dirac point [51,55,56]. Therefore, the proposed triply resonant scattering is valid in view of non-zero electronic states near Dirac point.

Figure 5(a) shows the carrier dynamics measured at 800 nm pump/3.15 μm probe (ν = 3175 cm^{-1}). After photoexcitation, a strong negative $\Delta T/T$, i.e. induced absorption, appears instantaneously and immediately turns into a positive $\Delta T/T$. In the following, the positive signal shows two time domains similar to the decay processes at other frequencies (Fig. 3(a)). For the curve fitting, three exponential functions were used with a convoluted instrument response function as shown in Fig. 5(a). It is worth noting that the fitting parameter τ_0 = 30 fs (smaller than our time resolution of 100 fs) is indicative of an ultrafast process. In other words, it is an instantaneous process which starts from the pump/probe early stage. Moreover, it is noted that the probe phonon frequency is approximately twice of that for G phonon (Fig. 5(b)). The typical electronic relaxation by G phonons shown in Fig. 3(c) is an intravalley intraband scattering. By examining the $\Delta T/T$ response in time scale and the phonon-related frequency, the ultrafast negative $\Delta T/T$ signal was attributed to a stimulated two-phonon emission process by resonant e-op scattering. Note that the sign flip of the signal in our case occurs instantaneously. Moreover, it is only observed at the specific probe frequency which is related to optical phonons. It is different from the previous studies [13,14,21,57], where the sign flip occurs after the decay of the transient differential transmission signal, *i.e.* 0.3-2 ps after photoexcitation. It could be caused by shrinkage of band separation [13], band structure renormalization [14] or residue materials [57].

At high intensities of the incident radiation, the pump photons excite large number of electrons from the VB (E_{puv}) to the CB (E_{puv}) (Fig. 5(d)). Initial stage of relaxation results in generating of considerable amount of optical phonons. Meanwhile, another intense MIR probe beam produces population inversion of electrons and holes at the probe excited levels E_{prc} and E_{prv}, in CB and VB, respectively. Emitted G phonons (in pairs) stimulate electronic transitions from E_{prc} to E_{prv} when $\nu_{pr} = c/\lambda_{pr}$ of the probe beam equals to 3175cm^{-1}, i.e. corresponds to second order of G phonons. We produce population inversion and, as a result, achieve amplification *via* stimulated emission of phonons. Correspondingly, the *band filling effect* caused by the intense probe beam weakens at E_{prc} and E_{prv}. In the kinetic curve (Fig. 5(a)) it leads to increase of absorption (negative change of transparency) promptly after the excitation pulse.

#176199 - $15.00 USD Received 13 Sep 2012; revised 18 Oct 2012; accepted 21 Oct 2012; published 5 Nov 2012

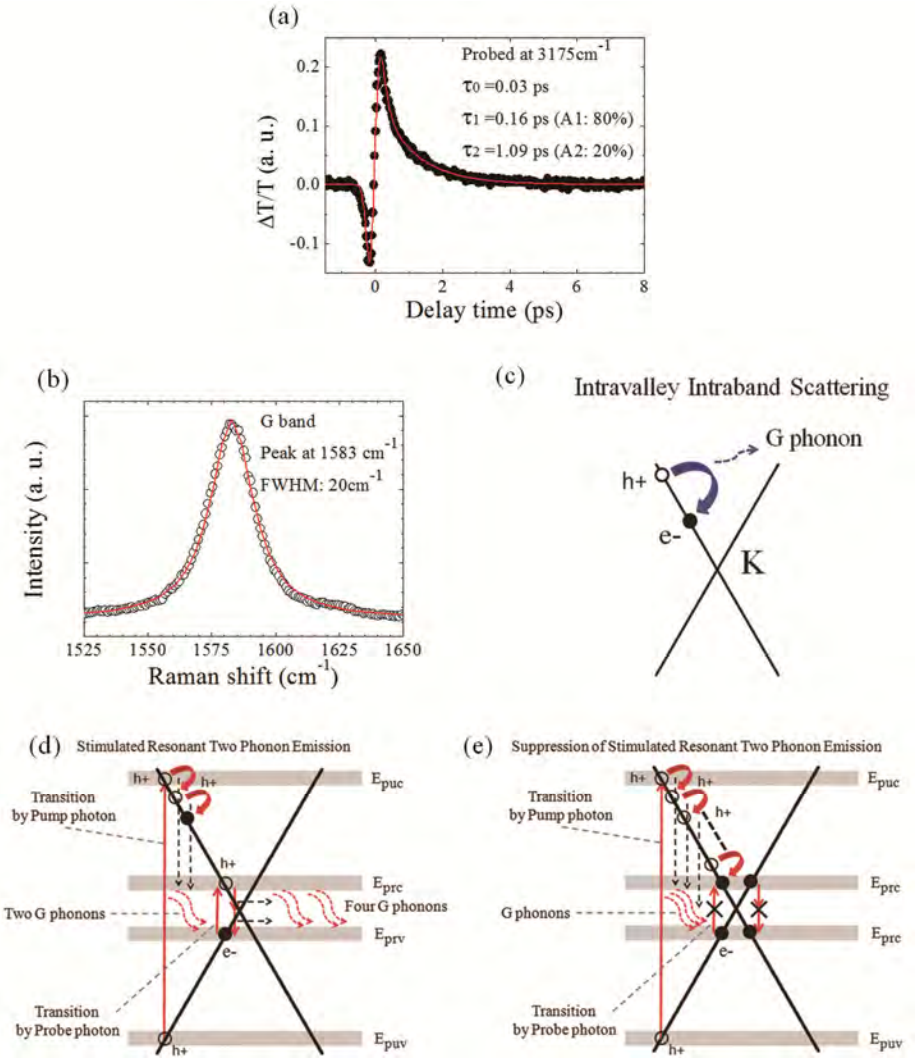

Fig. 5. (a) Carrier dynamics of graphene films at the probe frequency of 3175 cm^{-1} measured by the 800 nm pump/MIR probe setup; (b) Raman spectrum of G band of graphene films on CaF_2; (c) Electron relaxation by intravalley intraband e-op scattering in graphene; (d) Stimulated two phonon emission is at 3175 cm^{-1}; (e) Suppression of stimulated two phonon emission is at 3175 cm^{-1}.

When the electron population relaxes to the E_{prc} level, stimulated resonant two-phonon emission is suppressed as shown in Fig. 5(e). Electronic transitions are strongly restricted due to the Pauli blocking between E_{prc} and E_{prv} levels. After this, the ΔT/T signal becomes positive, which indicates the induced transmission (bleaching). Subsequently, the decay shows similar behavior as those in Fig. 3(a). Besides, Saito *et al.* [35] have also theoretically predicted a two-phonon Raman process with a phonon frequency of 3170 cm^{-1} after photoexcitation, which is consistent with our observation. Stimulated phonon emission has also been observed in Ruby [58–61] and few other materials [62–65]. Recently, the possibility of population inversion in photoexcited graphene was theoretically confirmed by performing microscopic calculations [66]. Population inversion in graphene under femtosecond excitation was also produced by Li *et al* [67] by observing stimulated emission in NIR. Our observations of stimulated phonon emission in graphene may lead to promising applications, e.g., a stimulated phonon source, saser [61] or phonon laser [62].

#176199 - $15.00 USD Received 13 Sep 2012; revised 18 Oct 2012; accepted 21 Oct 2012; published 5 Nov 2012

3. Methods

Monolayer graphene was grown on 25 μm thick copper foil (Purity 99.999%, Alfa Aesar) at 1000 °C by low-pressure chemical vapor deposition (CVD). After that, the graphene films on a 2 mm thick CaF_2 wafer were formed by transferring and stacking monolayer graphene films layer by layer. The details of graphene growth and transfer processes have been described in previous studies [13,47]. To collect strong differential transmission (ΔT/T) signals during the following pump-probe measurements, stacked graphene films were used here, rather than monolayer graphene.

Steady state transmission spectra were taken by a UV-Vis spectrophotometer (Cary 100Bio, Varian) and a Fourier transform IR spectrometer (Bruker Optics) with a mercury cadmium telluride (MCT) detector. A micro-Raman system (Reinshaw inVia) with a 532 nm excitation laser was used for measuring the Raman spectra. For the pump-probe measurements, a titanium-sapphire laser system (Coherent, Legend) was used as a pulse laser source: wavelength 800 nm, pulse width 150 fs, pulse repetition rate 1 kHz, and average power 1 W. The output of this system was used to pump an optical parametric amplifier (type II OPA; 4 mm β-BaB_2O_4). The resultant signal at about 1.2 μm and idler pulses at about 2 μm are utilized to generate 1 kHz tunable MIR pulses *via* different frequency mixing process in a 2 mm $AgGaS_2$ crystal. The degenerate MIR pump-probe experimental configuration at 2000 cm^{-1} has been described in a previous report in detail [68]. For the non-degenerate pump-probe setup, the 800 nm laser pulses (pulse energy, ~2 μJ) from the titanium-sapphire laser system are directly used as the pump beam and the *intense* MIR laser pulses (pulse energy, 1 - 2 μJ) at six frequencies (2600, 2700, 2800, 3000, 3100 and 3175 cm^{-1}) were selected as probe beams, respectively. The pump fluence is ~100 mJ/cm^2 and the excited carrier density is ~$10^{17}/cm^2$. The pulse widths of pump and probe are 150 and 230 fs, respectively. The cross-correlation functions in the MIR probe region are 280 ± 50 fs. The experimental data were fitted to a decay function convoluted with the cross-correlation function [13,69]. The overall time resolution of the experimental setup was 100 fs.

4. Conclusion

Ultrafast pump/MIR probe measurements of carrier dynamics have been studied in graphene films on CaF_2. Two decay processes were observed. The fast component is ~0.2 ps, which is attributed to the mixture of initial few ultrafast decay channels including interband and/or intraband e-op scattering, plasmon scattering, Auger scattering and impact ionization. The slow component is ~1.5 ps, which is substantially assigned to op-ap scattering. Furthermore, the frequency-dependent carrier relaxation was found, where the contribution of fast component was enhanced with the increase of the frequency of the MIR probe beam. At the probe frequency of 2700 cm^{-1}, the accelerated carrier relaxation was detected in the differential transmission kinetic curve, which resulted from the interband intervalley triple resonance e-op scattering in graphene. More interestingly, at the probe frequency of 3175cm^{-1}, an instant negative differential transmission was observed in the decay kinetics. This signal reflects a stimulated resonant two phonon emission process involved with zone-center G phonons in graphene. Our finding indicates an important potential application of graphene as a source of coherent ultrafast sound-wave emission.

Acknowledgments

We are grateful to Professor Maria-Elisabeth Michel-Beyerle for continuous support. We thank Ms Lin Ma, Dr. Zhiqiang Luo, and Mr. Jiaxu Yan for their suggestions and useful discussions. We thank Prof. Cesare Soci and Mr. Zilong Wang for their help with the steady-state infrared absorption measurement. Yu thanks the support of the Singapore National Research Foundation under NRF Award No. NRF-RF2010-07 and MOE Tier 2 MOE2009-T2-1-037.